Processing and Application of Ceramics 19 [1] (2025) 36–41
https://doi.org/10.2298/PAC2501036H

Structure and conductivity of Mn-doped $Na_3Zr_2Si_2PO_{12}$ solid electrolytes for sodium solid-state batteries

Shihang Hu, Jie Chang, Yazhou Kong*, Xuemei Liu*, Ru Yang, Jinquan Wang, Hao Sun, Kailong Zhang, Guang Hu, Weiwei Hu, Jiadong Zhang, Kun Hong

National & Local Joint Engineering Research Center for Mineral Salt Deep Utilization, Faculty of Chemical Engineering, Huaiyin Institute of Technology, Huaian 223003, P.R. China

Received 3 October 2024; Received in revised form 6 January 2025; Accepted 15 February 2025

Abstract

In the development of battery industry, all-solid-state batteries (ASSB) are considered as a substitution for conventional lithium battery with various advantages. Na super ion conductor (NASICON) is one of the most promising solid electrolytes for producing ASSBs. In this study, solid-state reaction method was used to perform Mn^{4+} doping into the popular solid-state electrolyte $Na_3Zr_2Si_2PO_{12}$ (NZSP) system, with the main goal to improve the electrolyte structure and electrical properties. The XRD results confirmed that NASCION structure still maintained in the sample, but some impurities were produced including Na_2CO_3 and $Zr(HPO_4)_2$. AC impedance results showed that certain amount of Mn-doping is beneficial for improving the room temperature conductivity of NZSP. The optimal doping amount of Mn is 4 at.%. Thus, the $Na_3Zr_{1.92}Mn_{0.08}Si_2PO_{12}$ sample exhibited the highest conductivity of 7.01×10^{-5} S/cm at room temperature with a low activation energy of 0.20 eV. DC polarization proved that the sample keeps the properties of ion conductor.

Keywords: *NASCION, Mn doping, solid electrolyte, structure, conductivity*

I. Introduction

Currently, lithium-ion batteries are widely used in various industries around the world mainly including automotives, cell phones, environmental protection, etc. [1]. However, there are some drawbacks existing in conventional lithium-ion batteries such as the limited resources or the safety risk, especially the fire hazard of the liquid electrolytes [1]. Therefore, the sodium-ion solid-state batteries begin to emerge into the horizon recent years, which is promising for the future battery industry with their outstanding safety performance and competitive electrochemical properties, especially the low cost and accessibility [2]. There are serval popular solid-state electrolyte systems including β-Al_2O_3, sulphide, polymers etc. [3]. Among them, sodium superionic conductor (NASICON) with the compounds structure ($Na_{1+n}Zr_2Si_nP_{3-n}O_{12}$, $0 \leq n \leq 3$), discovered by Hong *et al.* [4,5], is one of the most worth-researching candidates [6] with high thermal and chemical stability and high mechanical strength.

Improving the performance of NZSP by modification is of great significance for the development of Na solid-state batteries [7]. Cation substitution is considered as a potential approach to optimize the material [8]. Introduction of ions with different radii on Zr^{4+} position, such as: Sc^{3+} (0.74 Å), Y^{3+} (0.89 Å), Ca^{2+} (1.0 Å), La^{3+} (1.06 Å), Sr^{2+} (1.18 Å) [8–10] and so on, is a promising method to expand the ion channel and concentration of Na^+. Zhang *et al.* [11] introduced La^{3+} ions into the boundary of $Na_3Zr_2Si_2PO_{12}$ to form new phases ($Na_3La(PO_4)_2$, La_2O_3 and $LaPO_4$) enhancing the performance of the battery. He *et al.* [12] doped Mg^{2+} into $Na_3Zr_2Si_2PO_{12}$, improving the boundary of the electrolyte and the conductivity significantly. Jin *et al.* [13] provided different amounts of Na_2SiO_3 additive, and the addition of 5 wt.% Na_2SiO_3 had shown the highest total ionic conductivity of 1.45×10^{-3} S/cm at room temperature. Other ions including Ni^{2+} [14], Zn^{2+} [15] and Nb^{5+} [16] have already been doped in NZSP, and a high ionic conductivity of up to 3.4×10^{-3} S/cm at room temperature was obtained.

* Corresponding authors: tel: +86 15202588608,
e-mail: *kongyazhou@hyit.edu.cn* (Y. Kong)
liuxm7826@163.com (X. Liu)

In this paper, Mn^{4+} was doped into $Na_3Zr_2Si_2PO_{12}$ ceramic matrix to improve its electrical performance (Mn^{4+} and Zr^{4+} have the same valence and ionic radii of 0.54 and 0.72 Å, respectively). The structure and electrical conductivity of modified $Na_3Zr_2Si_2PO_{12}$ composite ceramics were measured by X-ray diffraction, scanning electron microscopy, AC impedance and DC polarization.

II. Experimental

Mn-doped NASICON ceramics were prepared via a simple solid-state reaction method with the reference to Huang *et al.* [17–19]. Na_2CO_3 (≥99.8%, Xilong Scientific), ZrO_2 (≥99.0%, Yongda Chemical), SiO_2 (≥99.0%, Xilong Scientific) and $NH_4H_2PO_4$ (≥99.0%, Yongda Chemical) powders were used as raw materials, which were weighted according to the stoichiometric formula of $Na_3Zr_{2-x}Mn_xSi_2PO_{12}$ ($0 \leq x \leq 2$). Excess of Na_2CO_3 and $NH_4H_2PO_4$ of 15 wt.% were added into the samples, compensating for the evaporation and the loss during the high-temperature synthesis process. Four groups of samples, where Mn^{4+} substituting Zr^{4+} in different amounts, were prepared, i.e. $Na_3Zr_{1.98}Mn_{0.02}Si_2PO_{12}$, $Na_3Zr_{1.95}Mn_{0.05}Si_2PO_{12}$, $Na_3Zr_{1.92}Mn_{0.08}Si_2PO_{12}$ and $Na_3Zr_{1.9}Mn_{0.1}Si_2PO_{12}$, and denoted as NZSP-0.02Mn, NZSP-0.05Mn, NZSP-0.08Mn and NZSP-0.10Mn, respectively (together with NZSP-0Mn as a reference sample). Firstly, the ball mill grinding was applied to mix the raw materials at the speed of 250 rpm for 4 h. Then the obtained mixture was dried at 65 °C for 6 h and calcined at 900 °C in muffle furnace for 12 h. Subsequently, the obtained samples were re-ground into powder and pressed into pellet with a 1.5 cm diameter under a pressure of 10 MPa. Finally, the samples were put into the muffle furnace and sintered at 1150 °C for 12 h.

Structure of the Mn-doped $Na_3Zr_2Si_2PO_{12}$ ceramic samples was analysed by X-ray diffraction (XRD, D8Discover, German) in the scan range from 10° to 70°. Scanning electron microscopy (SEM, S-3000N, Japan) technique was used to examine the micromorphology of the Mn-doped $Na_3Zr_2Si_2PO_{12}$ ceramic pellets. AC impedance (HP 4192A) analysis was carried out over 25–100 °C and DC polarization analysis (ADCMT 6243R) was carried out under 2 V for 3600 s at 25 °C.

III. Results and discussion

XRD patterns of the Mn-doped NASICON ceramics pellets sintered at 1150 °C are presented in Fig. 1. The main peaks of the sample correspond to $Na_3Zr_2Si_2PO_{12}$ phase (PDF #33-1313). Compared with the standard PDF card, the pattern drifts slightly to the left, which indicates the success of Mn^{4+} doping. The ionic radii of Na^+, Zr^{4+} and Si^{4+} are about 102, 79 and 42 pm, respectively, whereas the ionic radii of Mn^{2+} and Mn^{3+} are 83 and 67 pm, respectively. It is known from the XRD plots that the left shift of the peaks indicates the doping of large radius ions into small radius ion positions, which is in agreement with the proposed substitution of Zr^{4+} with Mn^{4+} ions. The pattern also shows the presence of impurities including $Zr(HPO_4)_2$ and Na_2CO_3, which can be found through comparing with the standard peak in test software. The intensities of the XRD peaks reveal the crystallization of the sample and demonstrate that the doping aids the crystallization. Thus, the intensity of the XRD peaks of the NZSP-0.08Mn sample is the strongest among all samples, which indicates that this sample has the highest crystallinity.

Figure 2 shows the fracture morphologies of the Mn-doped NZSP electrolytes. The dense structure can be observed in the NZSP and Mn-doped NZSP ceramic samples. It can be seen from Fig. 2e that the grain size distribution of the NZSP ceramics is inhomogeneous. SEM images of the Mn-doped NZSP ceramics (Figs. 2a-d) show uniform microstructure compared with the reference NZSP sample. It can be observed that average grain size in the samples sintered at 1150 °C is 5–10 μm. The dense structure proves that the doping Mn into the NZSP has beneficial influence on sintering process.

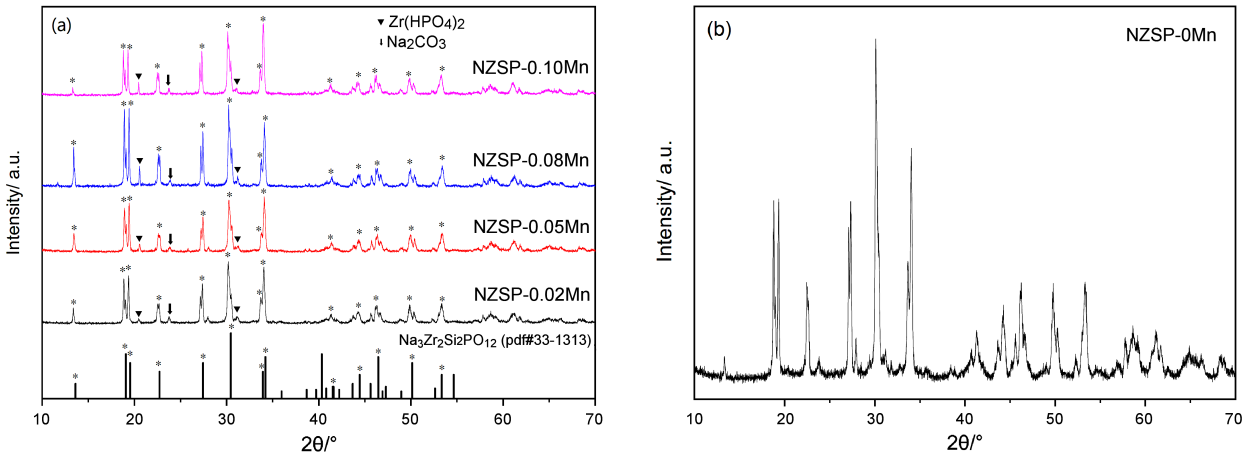

Figure 1. XRD patterns of: a) Mn doped NZSP and b) pure NZSP ceramic pellets sintered at 1150 °C

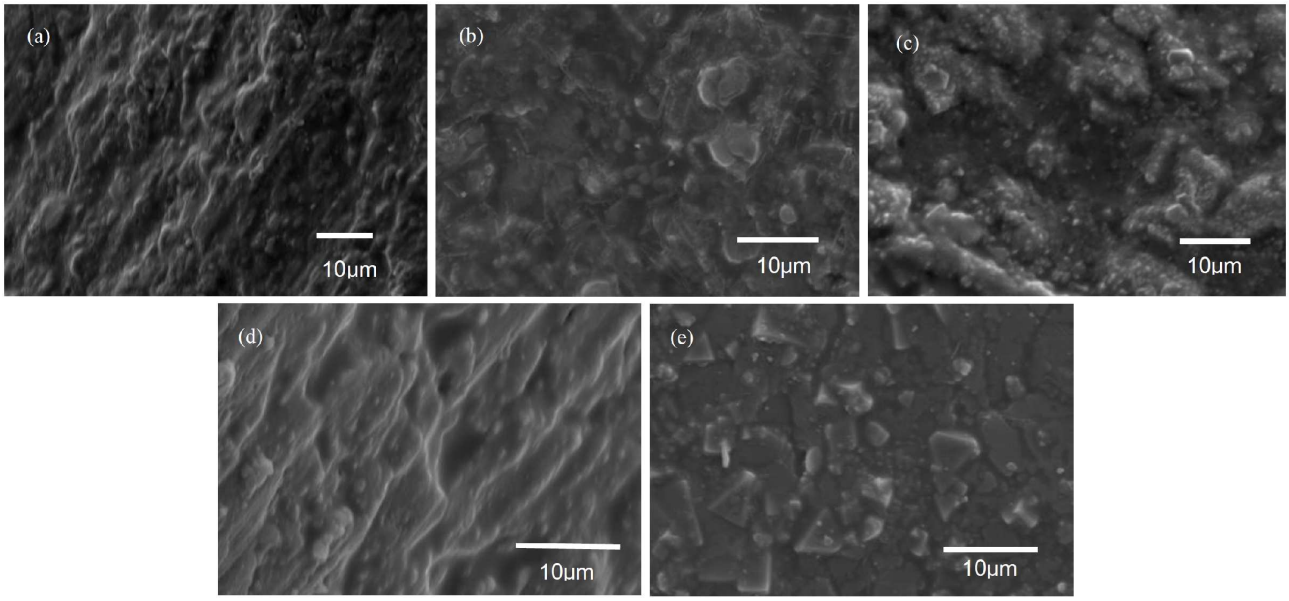

Figure 2. SEM images of the sintered electrolytes: a) NZSP-0.02Mn, b) NZSP-0.05Mn, c) NZSP-0.08Mn, d) NZSP-0.10Mn and e) NZSP-0Mn

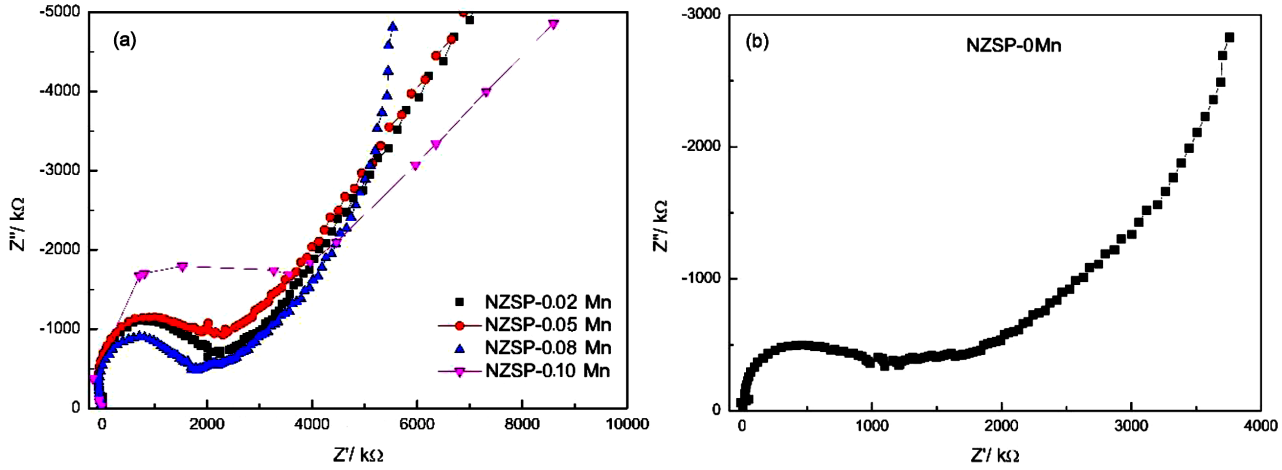

Figure 3. Nyquist plots of ceramic pellets: a) NZSP-0.02Mn, NZSP-0.05Mn, NZSP-0.08Mn, NZSP-0.10Mn and b) NZSP-0Mn

Figure 3 shows the results of AC impedance analysis. Before the test every pellet was covered by graphite on both sides to act as electrode. Graphite is a typical Na^+ blocking electrode. The sample was all set in an incubator to create a stale-temperature environment. The standard graph of every ceramic sample contains a semicircle in high frequency range and an oblique line in low frequency range. The intersection with the real x-axis represents the total resistance of the sample (R). The intersection of the NZSP-0.08Mn electrolyte was found to be the smallest among all samples, which means this sample has low resistance and high ionic conductivity.

The total conductivity σ of each sample was calculated by using the following formula:

$$\sigma = \frac{d}{R \cdot S} \tag{1}$$

where d is the thickness of ceramic pellet and S is the single-surface area of carbon electrode on the pellet. The results were listed in Table 1. The conductivity of the NZSP-0Mn sample is 6.28×10^{-5} S/cm at room temperature. The conductivity of the NZSP-0.08Mn is the highest, i.e. 7.01×10^{-5} S/cm, while the NZSP-0.02Mn, NZSP-0.05Mn, NZSP-0.10Mn electrolytes have conductivities of 5.86×10^{-5}, 5.45×10^{-5} and 3.71×10^{-5} S/cm, respectively. According to the literature data [20] the maximum total conductivity of Ge-doped NA-

Table 1. Conductivity and activation energy of ceramic samples

Sample	σ_{total} [S/cm]	σ_{ele} [S/cm]	E_a eV]
NZSP-0Mn	6.28×10^{-5}	6.57×10^{-10}	0.15
NZSP-0.02Mn	5.86×10^{-5}	2.80×10^{-7}	0.22
NZSP-0.05Mn	5.45×10^{-5}	9.78×10^{-8}	0.24
NZSP-0.08Mn	7.01×10^{-5}	2.62×10^{-7}	0.20
NZSP-0.10Mn	3.71×10^{-5}	1.05×10^{-7}	0.10

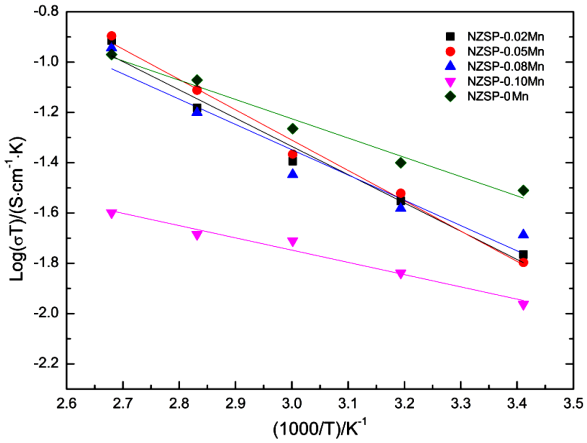

Figure 4. The Arrhenius plots of conductivity for ceramic pellets

SICON at room temperature was 1.4×10^{-3} S/cm. On the other hand, by partially replacing Zr^{4+} with Ca^{2+}, the conductivity of Ca-doped NZSP (prepared by sol-gel method and sintering) was improved to 1.67×10^{-3} S/cm [21,22].

Figure 4 shows the Arrhenius plots of all ceramic pellets. The conductivity of samples was measured at different temperatures (40, 60, 80 and 100 °C). The activation energy can be obtained from the measured data by using the Arrhenius equation:

$$\sigma \cdot T = \sigma_0 \exp\left(-\frac{E_a}{K_B \cdot T_0}\right) \tag{2}$$

The natural logarithm on both sides gives:

$$\ln(\sigma \cdot T) = \ln \sigma_0 - \frac{E_a}{K_B \cdot T_0} \tag{3}$$

Setting $y = \ln(\sigma \cdot T)$ and $K = 1/(K_B \cdot T)$ yields:

$$y = A - E_a \cdot K \tag{4}$$

where σ is the conductivity of the sample, T the temperature, σ_0 denotes the finger forward factor, E_a is the activation energy, K_B is the Boltzmann constant and T_0 is the initial temperature.

Activation energies of the ceramic samples are listed in Table 1. The activation energy values range from 0.15 to 0.24 eV which are comparable with the traditional solid electrolyte. The NZSP-0.05Mn ceramics has the highest activation energy of 0.24 eV and the NZSP-0.10Mn electrolyte has the lowest activation energy of 0.10 eV, which is not much different from that of the NZSP-0Mn sample. The results show that Mn-doping did not significantly affect the activation energy, but is beneficial to improve the electrical properties of the NZSP ceramics.

An optimal solid electrolyte should have a low electronic conductivity to avoid short circuit through electrolyte. Figure 5 shows the DC polarization plots for the electronic conductivity of the prepared ceramics. With the increase of polarization time, the current of every pellet decreases continuously. The current still keeps a steady state after 3600 s. Electronic conductivity can be calculated by the following equation:

$$\sigma_{ele} \frac{d \cdot I}{S \cdot U} \tag{5}$$

where σ_{ele} is electronic conductivity, d is the thickness of ceramic pellet, I is the final steady state current shown in Fig. 5 and U is the polarization voltage applied for the test (5 V in this experiment). The results presented in Table 1 confirm that Mn-doping obviously improves the electronic conductivity and for the NZSP-0.02Mn, NZSP-0.05Mn, NZSP-0.08Mn and NZSP-0.10Mn samples the electronic conductivity accounted for 0.48%, 0.18%, 0.37% and 0.28% of the total conductivity, respectively, whereas the NZSP-0Mn only accounted for 0.001%. This is a bad effect for a solid electrolyte. However, this proportion is still three orders of magnitude lower than the total conductivity and this indicates that Mn doped NZSP ceramics are still mainly an ion conductor.

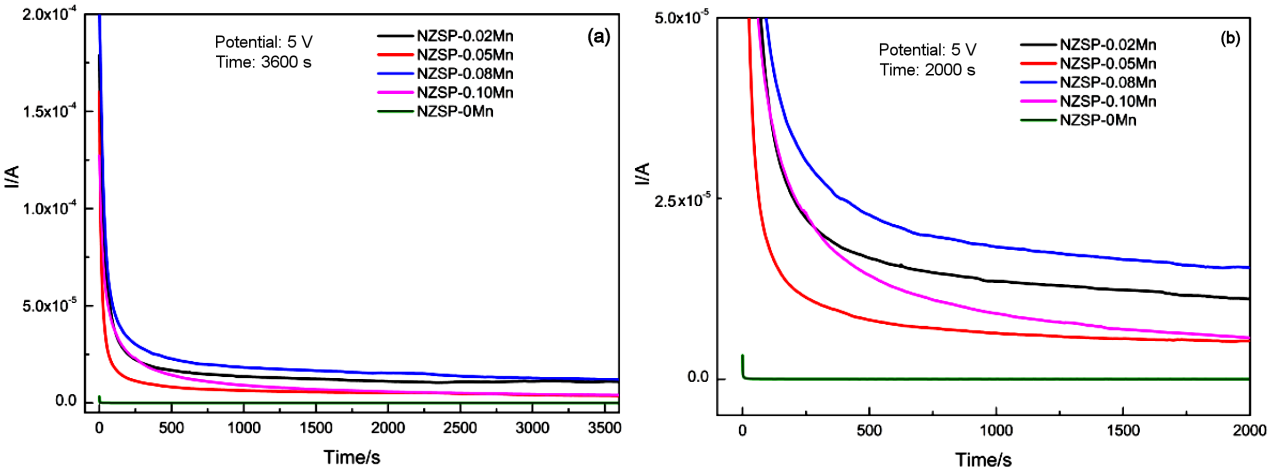

Figure 5. DC polarization current-time curves of NZSP-0.02Mn, NZSP-0.05Mn, NZSP-0.08Mn, NZSP-0.10Mn and NZSP-0Mn ceramics

IV. Conclusions

This paper studied the effect of Mn^{4+} doping into $Na_3Zr_2Si_2PO_{12}$ solid electrolyte material and the enhancement of the ionic conductivity, morphology and microstructure. XRD results confirm that the main peaks of the sintered sample correspond to $Na_3Zr_2Si_2PO_{12}$ phase and are slightly shifted to the left indicating successful Mn-doping. The dense structure in the Mn-doped NZSP ceramic samples was observed by SEM. It can be found that the modification with Mn^{4+} ions promotes the ionic conductivity up to 7.01×10^{-5} S/cm and gives low activation energy of 0.20 eV. DC polarization indicates that, even doping obviously improves the electronic conductivity, the Mn-doped NZSP ceramics are still ion conductor. This co-assisting method provides a promising strategy for further research about improving the ionic conductivity of solid electrolyte, which is beneficial for the development of all-solid-state batteries.

Acknowledgement: This work was supported by the fund of National & Local Joint Engineering Research Center for Mineral Salt Deep Utilization (SF202206), Natural Science Foundation of the Higher Education Institutions of Jiangsu Province (23KJB450001), Jiangsu University students innovation and entrepreneurship training program (202311049018Z), Foundation of Key Laboratory for Palygorskite Science and Applied Technology of Jiangsu Province (HPZ202201).

References

1. H.L. Yang, B.W. Zhang, K. Konstantinov, Y.X. Wang, H.K. Liu, S.X. Dou, "Progress and challenges for all-solid-state sodium batteries", *Adv. Energ. Sust. Res.*, **2** [2] (2021) 2000057.
2. N. Yabuuchi, K. Kubota, M. Dahbi, S. Komaba, "Research development on sodium ion batteries", *Chem. Rev.*, **114** [23] (2014) 11636–11682.
3. K.B. Hueso, V. Palomares, M. Armand, T. Rojo, "Challenges and perspectives on high and intermediate-temperature sodium batteries", *Nano Res.*, **10** [12] (2017) 4082–4114.
4. H.Y-P. Hong, "Crystal structures and crystal chemistry in the system $Na_{1+x}Zr_2Si_xP_{3-x}O_{12}$", *Mater. Res. Bull.*, **11** [2] (1976) 173–182.
5. J.B. Goodenough, H.Y-P. Hong, J.A. Kafalas, "Fast Na^+-ion transport in skeleton structures", *Mater. Res. Bull.*, **11** [2] (1976) 203–220.
6. Y. Li, H. Xu, P.H. Chien, N. Wu, S. Xin, L. Xue, K. Park, Y.Y. Hu, J.B. Goodenough, "A perovskite electrolyte that is stable in moist air for lithium-ion batteries", *Angew. Chem Int. Edit.*, **57** [2] (2018) 8587–8591.
7. Y.B. Rao, K.K. Bharathi, L.N. Patro, "Review on the synthesis and doping strategies in enhancing the Na ion conductivity of $Na_3Zr_2Si_2PO_{12}$ (NASICON) based solid electrolytes", *Solid State Ionics*, **366–367** (2021) 115671.
8. S. Song, H.M. Duong, A.M. Korsunsky, N. Hu, L. Lu, "A Na^+ superionic conductor for room-temperature sodium batteries", *Sci. Rep.*, **6** (2016) 32330.
9. Q.L. Ma, M. Guin, S. Naqash, C.L. Tsai, F. Tietz, O. Guillon, "Scandium-substituted $Na_3Zr_2(SiO_4)_2(PO_4)$ prepared by a solution-assisted solid-state reaction method as sodium-ion conductors", *Chem. Mater.*, **28** [13] (2016) 4821–4828.
10. Y.L. Ruan, S.D. Song, J.J. Liu, P. Liu, B.W. Cheng, X.Y. Song, V. Battaglia, "Improved structural stability and ionic conductivity of $Na_3Zr_2Si_2PO_{12}$ solid electrolyte by rare earth metal substitutions", *Ceram. Int.*, **43** [10] (2017) 7810–7815.
11. Z.Z. Zhang, Q.H. Zhang, J.N. Shi, Y.S. Chu, X.Q. Yu, K.Q. Xu, M.Y. Ge, H.F. Yan, W.J. Li, L. Gu, Y.S. Hu, H. Li, X.Q. Yang, L.Q. Chen, X.J. Huang, "A self-forming composite electrolyte for solid-state sodium battery with ultralong cycle life", *Adv. Energy Mater.*, **7** [4] (2017) 1601196.
12. S. He, Y. Xu, X. Ma, Y. Chen, J. Lin, C. Wang, "Mg^{2+}/F^- synergy to enhance the ionic conductivity of $Na_3Zr_2Si_2PO_{12}$ solid electrolyte for solid-state sodium batteries", *ChemElectroChem*, **7** [9] (2020) 2087–2094.
13. J.A.S. Oh, L. He, A. Plewa, M. Morita, Y. Zhao, T. Sakamoto, X. Song, W. Zhai, K.Y. Zeng, L. Lu, "Composite NASICON ($Na_3Zr_2Si_2PO_{12}$) solid-state electrolyte with enhanced Na^+ ionic conductivity: Effect of liquid phase sintering", *ACS Appl. Mater. Interfaces*, **11** [43] (2019) 40125–40133.
14. M. Samiee, B. Radhakrishnan, Z. Rice, Z. Deng, Y.S. Meng, S.P. Ong, J. Luo, "Divalent-doped $Na_3Zr_2Si_2PO_{12}$ natrium superionic conductor: Improving the ionic conductivity via simultaneously optimizing the phase and chemistry of the primary and secondary phases", *J. Power Sources*, **347** (2017) 229–237.
15. Z. Zhang, Q. Zhang, J. Shi, Y.S. Chu, X. Yu, K. Xu, M. Ge, H. Yan, W. Li, L. Gu, Y.S. Hu, H. Li, X.Q. Yang, L. Chen, X. Huang, "A self-forming composite electrolyte for solid-state sodium battery with ultralong cycle life", *Adv. Energy Mater.*, **7** [4] (2017) 1601196.
16. J. Yang, G. Liu, M. Avdeev, H. Wan, F. Han, L. Shen, Z. Zou, S. Shi, Y.-S. Hu, C. Wang, X. Yao, "Ultrastable all-solid-state sodium rechargeable batteries", *ACS Energy Lett.*, **5** [9] (2020) 2835–2841.
17. X. Huang, J.W. Tang, Y.J. Zhou, K. Rui, X. Ao, Y. Yang, B.B. Tian, "Developing preparation craft platform for solid electrolytes containing volatile components: experimental study of competition between lithium loss and densification in $Li_7La_3Zr_2O_{12}$", *ACS Appl. Mater. Interfaces*, **14** [29] (2022) 33340–33354.
18. X. Huang, Y. Lu, Z. Song, K. Rui, Q.S. Wang, T.P. Xiu, M.E. Badding, Z.Y Wen, "Manipulating Li_2O atmosphere for sintering dense $Li_7La_3Zr_2O_{12}$ solid electrolyte", *Energy Storage Mater.*, **22** (2019) 207–217.
19. L. Wang, Z.Y. Zhou, X. Yan, F. Hou, L. Wen, W.B. Luo, J. Liang, S.X. Dou, "Engineering of lithium-metal anodes towards a safe and stable battery", *Energy Storage Mater.*, **14** (2018) 24–48.
20. Z. Zhang, Z. Zou, K. Kaup, R. Xiao, S. Shi, M. Avdeev, L. Chen, "Correlated migration invokes higher Na^+-ion conductivity in NaSICON-type solid electrolytes", *Adv. Energy Mater.*, **9** [42] (2019) 1902373.
21. Y. Lu, J.A. Alonso, Q. Yi, L. Lu, Z.L. Wang, C. Sun, "A high-performance monolithic solid-state sodium battery with Ca^{2+} doped $Na_3Zr_2Si_2PO_{12}$ electrolyte", *Adv. Energy Mater.*, **9** [28] (2019) 1901205.

22. Y. Kong, G. Hu, K. Zhang, W. Hu, "Conductivity and electrochemical stability of Li^+ substituted high-entropy $Li_x(Mg_{0.2}Co_{0.2}Ni_{0.2}Cu_{0.2}Zn_{0.2})_{1-0.5x}O$ ceramics", *Process. Appl. Ceram.*, **16** [3] (2022) 201–206.